# Microscopic study of $1/f$ noise in metal nanobridges

K. S. Ralls
*AT&T Bell Laboratories, Murray Hill, New Jersey 07974*

R. A. Buhrman
*School of Applied and Engineering Physics, Cornell University, Ithaca, New York 14853-2501*
(Received 14 February 1991)

Extensive studies of $1/f$ noise and its microscopic constituents have been conducted in clean metal nanobridges 3–40 nm wide. The resistance noise results from the fluctuation of metastable defects between discrete configurations; at low temperatures, activation energies, scattering cross-section changes, and attempt times are measured. Interactions between defects dominate the high-temperature noise signal, and are, in fact, required to produce a $1/f$ noise signal. The measured interaction strength is too large to be explained by a simple model of fluctuating elastic dipoles interacting through the lattice strain field. The analysis suggests that collective reconfigurations of regions of a "defect glass" are responsible both for the discrete fluctuations and the strong interaction energy. Implications for more disordered systems are discussed.

## I. INTRODUCTION

The remarkable ubiquity of $1/f$ noise in both metal and nonmetal systems, independent of the microscopic details of the system, has spurred much interest in the field over the years. In semiconductor devices and tunnel junctions it has recently been possible to observe the individual components comprising the $1/f$ noise with samples larger than 0.1 $\mu$m.[1–4] Resolving the constituents of $1/f$ nose in metal films has proved to be much more difficult, however. This difficulty is readily understood if we make the usual assumption that such noise ultimately arises from fluctuations of atomic defects in the system. The much shorter screening length found in metals implies a much smaller scattering-cross-section change for a change of an individual defect in a metal than in a semiconductor system. The comparison is even more uneven when a tunneling system is considered since a defect change that results in the capture or emission of a charge in a tunnel barrier can have a much larger effect on the fractional conductance of the system than that caused by a defect motion or reorientation in a metal. But not only is it difficult to fabricate metal samples that are small enough to resolve the microscopic components of the $1/f$ noise, satisfactory characterization of sample size and cleanliness is also a daunting task. For this reason, to date, most studies of $1/f$ noise in clean metal films have concentrated by necessity on measurements of the noise power spectral density and higher-order moments. Although evidence has been accumulating that defect motion is indeed responsible for the $1/f$ noise found in metal films, the microscopic nature of the $1/f$ noise has not previously been established by direct observation.

In this paper we report results of extensive noise studies in well-characterized metal samples, which we refer to as metal nanobridges, whose minimum cross-sectional area is so small that an atomic-sized change in the key sample dimensions causes a readily measurable change in sample resistance. Using these nanobridges we have observed the transition, at room temperature, from bulklike $1/f$ noise in the largest samples, to a noise signal dominated by discrete, individual defect fluctuations in the smallest samples. These measurements confirm that defect motion is responsible for the $1/f$ noise found in clean metal films.[5] But perhaps more importantly we are able to obtain specific information about characteristic attempt frequencies, scattering-cross-section changes, and defect interactions. We find, not surprisingly, that the characteristic attempt times are generally of order $10^{-13}$ s, characteristic of atomic vibration, and that the scattering-cross-section changes are on the order of atomic dimensions. However, the strong interactions that we observe between defects and indeed the absence of any truly independent defects in these comparatively clean, crystalline metal films present a novel picture of $1/f$ noise in such systems, while providing new insight into the nature of $1/f$ noise and defect motion in more disordered systems.

We begin the paper with a brief overview of the field of $1/f$ noise in Sec. II. Section III contains a discussion of nanobridges, their fabrication and characterization, and the noise measurement technique. In Sec. IV we present the results of $1/f$ noise measurements in nanobridges. Here we show that the $1/f$ noise magnitude observed in the larger nanobridges scales correctly from bulk thin-film samples five orders of magnitude greater in volume. We also discuss the differences in the noise behavior for a variety of metals, the differences of which clearly reflect different defect distributions in the materials. In Sec. V we describe how in smaller nanobridges the $1/f$ noise can be resolved into its discrete components. Since these samples are in the local interference regime, the fluctuations show atomic-sized changes in the scattering cross-section, as expected. In Sec. VI we show examples of

 

simple interactions between defects, and present high-temperature (300 K) results that directly demonstrate that there is no such thing as an independent defect in these clean metal films. Indeed, defect interactions are fundamental to the production of a $1/f$ noise spectrum in metal films. The nature of this defect interaction is discussed in Sec. VII and the conclusion is drawn that the $1/f$ noise does not arise from the reorientation of simple dipolar defects. Rather, clustering defects interact through the elastic strain field sufficiently strongly to form a type of defect glass in which the defect potential seen by any one dipolar element is strongly affected by the fluctuation of any nearby defect elements. We conclude with a discussion of the possible implications of this work for advancing the understanding of more strongly disordered and amorphous systems.

## II. $1/f$ NOISE IN METAL FILMS

In a wide variety of metal and nonmetal systems, one finds what is known as generic $1/f$ noise, where the noise power spectral density $S_R \sim 1/f^{\alpha}$ with $0.8 < \alpha < 1.2$ over many decades in frequency. The standard model for obtaining a $1/f$ spectrum involves superposing many Lorentzian spectrum noise sources with a broad range of characteristic mean fluctuation times $\tau_i$,

$$S_R(f) = \sum_{i=1}^{N} \langle (\delta R^2) \rangle_i \frac{\tau_i}{1+\omega^2\tau_i^2} \ . \tag{1}$$

As long as the distribution of times spans many decades smoothly, this superposition produces generic $1/f$ noise, with a surprising lack of sensitivity to the details of the time distribution. The only restriction that this model places on the microscopic origin of the noise is that of Lorentzian spectrum noise sources, which implies that the noise can be described by a characteristic exponential relaxation time back to equilibrium. A Lorentzian spectrum results from a two-level fluctuation in which the time spent in the high or low state has an exponential distribution,[6] such as could plausibly be caused by reversible defect motion where the motion originates either by thermal activation or tunneling.

In considering $1/f$ noise in metal samples it is important to distinguish between two possible conduction regimes. These regimes are defined by whether the elastic-scattering, mean free path $\lambda_e$ is short or long when compared to the electron phase coherence length $\lambda_\phi$. In the former case one is in the universal conductance fluctuation regime, which has received a great deal of attention lately.[7,8] In this highly diffusive regime, for systems or subsystems with dimensions $\sim\lambda_\phi$, effects due to long-range electron interference can result in a change of the system conductance of order $e^2/h$ whenever a single atomic scale defect reorients itself enough to materially change its scattering cross section. But typical metal films, at or above 77 K, are in the other, cleaner limit ($\lambda_\phi < \lambda_e$), which is often termed the local interference regime. There the effect of elastic scattering is restricted to local interference of the electron wave function within an electron wavelength or so of the defect.[9] In this paper we will be discussing results that have been obtained solely with samples in this local interference regime.

As indicated above, for clean metal films in the local interference regime evidence has been accumulating over the years that defect motion is indeed responsible for the observed $1/f$ noise. A complete review of the field of $1/f$ noise has been published recently;[10] only a few seminal experiments will be discussed here before turning to a discussion of the results of $1/f$ and discrete low-frequency noise in metal nanobridges.

Pelz and Clarke[11] irradiated copper films and showed that the increase in the $1/f$ noise magnitude correlated well with the increase in sample resistivity. This showed quite clearly that excess $1/f$ noise in a sample can be caused by adding defects. Similarly Zimmerman and Webb[12] added $H^+$ to palladium films and showed that the $1/f$ noise magnitude observed at low temperatures correlated well with the $H^+$ density deduced from the diffusion noise signal found at higher temperatures. Neither of these experiments established the origin of the $1/f$ noise found in the samples before the addition of defects.

However, an extensive study of this "intrinsic" $1/f$ noise was carried out somewhat earlier by Dutta and Horn,[13] who studied the $1/f$ noise magnitude as a function of temperature in unadulterated, thermally evaporated polycrystalline metal films. Assuming thermally activated Lorentzian noise sources with a fluctuation attempt time of $10^{-13}$ s, characteristic of atomic vibrations, they deconvolved Eq. (1) to get the implicit distribution of activation energies, $D(\varepsilon_0) = fS_R(f)/[(\delta R)^2 kT]$. They often found that the distribution of energies was peaked around 1 eV, with the peak energy correlating reasonably well with expected activation energies for defects in the different materials they studied. Thus Dutta and Horn showed that the temperature dependence of the $1/f$ noise magnitude found in the metal films is consistent with defect motion being the microscopic mechanism.

Finally, although to date researchers have typically measured the noise power spectral density of metal samples, a clever technique exploited by Garfunkel and Weissman[10] has been to measure higher-order correlation functions. This technique, based on the fact that defect fluctuations should produce noticeably non-Gaussian noise, allows a search for this noise behavior in samples that are still too large to distinguish the individual fluctuations. So far, of the clean metals, only niobium and aluminum have displayed measurable non-Gaussian behavior in the relatively large ($10^{-15}$cm$^3$) samples used in these studies.

## III. EXPERIMENTAL PROCEDURE

The development of a thin-film fabrication technique for metal nanobridges, clean, stable "point contacts" as small as 10–20 atoms across, has now made it possible to study the individual constituents of $1/f$ noise in metal films. This fabrication process has been described in more detail elsewhere;[14] here we present a brief summary. Samples are fabricated by patterning a single 40-nm hole in poly(methyl methacrylate) on a 50-nm suspended sil-

icon nitride membrane using electron beam lithography. The pattern is transferred to the silicon nitride with a marginal reactive ion etch, in which the etch just breaks through the membrane. As a result, the opening on the far side of the membrane is much smaller than that actually patterned. Finally, the wafers are rotated to expose both sides while metal is evaporated, forming the nanobridge region in a single processing step. For the copper samples discussed extensively below, the bulk elastic mean free path is about 180 nm. A probable cross-sectional schematic of a nanobridge, to scale in the horizontal direction, is shown in Fig. 1. In the case of the copper films, the typical grain size of the polycrystalline films used in these nanobridge experiments is about 200 nm as measured by transmission electron microscopy (TEM). Examination of the nanobridge regions[14] by TEM also suggests that a single crystallite forms the nanobridge region, a fact that is confirmed by low-temperature electrical measurements as discussed below, and the very high stability of these structures against electromigration.[15]

Nanobridges are characterized using a measurement known as point-contact spectroscopy, in which the second derivative of the $I$-$V$ characteristic of a ballistic point contact yields a geometrical average of the product of the phonon density of states and the electron-phonon coupling strength. First discovered by Yanson,[16] point-contact spectroscopy has been used for over a decade to investigate energy-dependent scattering of electrons in a wide variety of systems.[17] The explanation presented here can be found in more detail in the review article by Jansen, van Gelder, and Wyder.[18] The resistance of a metal constriction can be divided fairly well into two parts, that due to scattering of electrons within the material and that due to electron flow restrictions imposed by sample geometry. In most metal thin-film samples the electron mean free path is small compared to the sample dimensions, and the latter term is negligible. However, for samples in the ballistic transport regime the geometrical resistance dominates, and the sample resistance becomes independent of the electron mean free path. Note that in this case the length scale over which the voltage drops is determined by the sample dimensions, not the electron mean free path. For a point-contact geometry, that of a small constriction between two bulk electrodes, one finds a mean-free-path-dependent, or diffusive, resistance

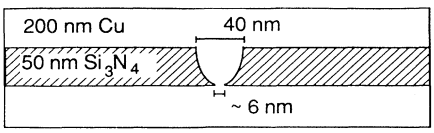


FIG. 1. Cross-sectional schematic of a metal nanobridge, to scale in the lateral dimension. The extremely small constriction at the lower side of the silicon nitride determines the sample volume over which an applied voltage drops.

$$R_D=\frac{\rho}{2c} \tag{2}$$

and a geometrical, or ballistic, resistance

$$R_B=\frac{4\rho\lambda}{3\pi c^2}\ , \tag{3}$$

where $\rho$ is the resistivity, $\lambda$ is the electron mean free path, and $c$ is the constriction radius. Since $\rho\sim 1/\lambda$, $R_B$ is of course independent of $\lambda$. Although the actual resistance for a sample with finite $\lambda$ is rather complicated, the resistance of a point contact is well approximated by the sum[18]

$$R\sim R_B+R_D=R_B\left[1+\frac{c}{\lambda}\right]\ . \tag{4}$$

The point-contact spectroscopy effect can be understood by considering that the increase in resistance of metal samples with increasing voltage, in the absence of sample heating, stems primarily from the decrease in the electron mean free path $\lambda$ due to increasing the number of channels for phonon emission. Even when the ballistic resistance is larger than the diffusive, or mean-free-path-dependent, resistance, $dR/dV$ is given by $dR_D/dV$, because the ballistic resistance is independent of the electron mean free path. Thus in both the diffusive and the ballistic transport regimes

$$\frac{dR}{dV}=\frac{dR_D}{dV}=R_D\lambda\frac{d}{dV}\left[\frac{1}{\lambda}\right]\ . \tag{5}$$

However, in the ballistic regime $1/\lambda$ has a very simple functional dependence on voltage, because the sample size is small compared to the electron mean free path. If an electron emits a phonon at all, it is much more likely to emit only a single phonon in traversing the sample than it is to emit more than one, and $d/dV(1/\lambda)$ is dominated by single-phonon emission events. Because electrons do not have time to equilibrate with the lattice while traversing the device, the electrons can lose up to $e$ times the voltage of energy in an inelastic-scattering event, so using Fermi's golden rule the scattering rate is given by

$$\frac{1}{\tau}=\frac{2\pi}{\hbar}\sum_{\mathbf{q},\mathbf{k},\mathbf{k}'}|g_{\mathbf{q}}|^2[\delta(\varepsilon_{\mathbf{k}'}-\varepsilon_{\mathbf{k}}-\hbar\omega_{\mathbf{q}})(1-f_{\mathbf{k}}) +\delta(\varepsilon_{\mathbf{k}'}-\varepsilon_{\mathbf{k}}+\hbar\omega_{\mathbf{q}})f_{\mathbf{k}}]\ , \tag{6}$$

where $g$ is the matrix element for electron-phonon scattering, $\mathbf{q}$ is the phonon wave vector, and $\mathbf{k},\mathbf{k}'$ are the initial and final electron wave vectors. The phonon density of states times the electron-phonon coupling strength, known as the Eliashberg function, is defined as

$$\alpha^2F(\varepsilon)=\frac{N_0}{2}\int\frac{q\,dq}{2k_f^2}|g_q|^2\delta(\varepsilon-\hbar\omega_q)\ , \tag{7}$$

so that, with some manipulation, the scattering rate at $T=0$ can be written as

$$\frac{1}{\tau(\varepsilon)}=2\pi\int_0^{\varepsilon}d\varepsilon\,\alpha^2F(\varepsilon)\ . \tag{8}$$

Now $\lambda \propto 1/\tau$, so using Eq. (5) we find the PCS result

$$\frac{dR}{dV} \propto \alpha^2 F(\omega) . \tag{9}$$

A typical phonon spectrum for one of the copper nanobridges is shown in Fig. 2. The large peak near 15 mV is due to transverse phonons, while the smaller peak near 30 mV is due to longitudinal phonons. The large phonon signal and the small "background" signal past 30 mV are characteristics of high-quality point-contact spectroscopy, indicative of a device in the ballistic transport regime. That is, the existence of a clean phonon spectrum is proof that most electrons have time to emit no more than one phonon while traversing the device. This means that the electron mean free path in the constriction region cannot be substantially shorter than that found in the bulk ($\lambda \sim 180$ nm). We also note that if, for example, there were significant numbers of magnetic scatterers in the structure, a zero-bias anomaly reflecting the Kondo effect would be apparent.[19]

It is also important to point out that the absence of any voltage-dependent structure at voltages below the first phonon peak demonstrates that the resistivity does not contribute significantly to the total resistance. This is because the sample dimensions are usually small or comparable to the electron phase coherence length and in a diffusive sample one would expect to see universal conductance fluctuation effects with changing sample voltage. But if the samples are also small compared to the elastic diffusive-scattering length, these effects disappear. Universal conductance fluctuation effects are, as discussed above, explained by calculations of the change in conductivity that results from a change in an individual scattering cross section, based on the assumption that most of the electron paths through the sample are diffusive. But if, as is the case for a ballistic nanobridge, the resistivity contributes only a very small fraction of the total sample resistance, then the universal conductance fluctuation effects should be reduced by the square (because the effect is a conductance fluctuation, not a resistance fluctuation) of that fraction from what one would otherwise expect based on the total sample resistance. Thus the absence of significant universal conductance fluctuation effects in the as-fabricated metal nanobridges further confirms the fact that the transport mechanism is a predominantly ballistic flow at low temperatures, so that even at low temperatures the samples are not in the universal conductance fluctuation regime. (In nanobridges that have been disordered by electromigration so as to have a larger diffusive component to the resistance, we do see universal conductance fluctuation effects of the expected magnitude. Transport and noise measurements on such samples will be reported elsewhere.[20]) Because the nanobridges, as fabricated, are not in the universal conductance fluctuation regime, we do not expect the amplitude of a fluctuation to change as the temperature changes $\lambda_\phi$ from being longer than the sample size to being shorter than the sample size. We have experimentally verified this expectation.

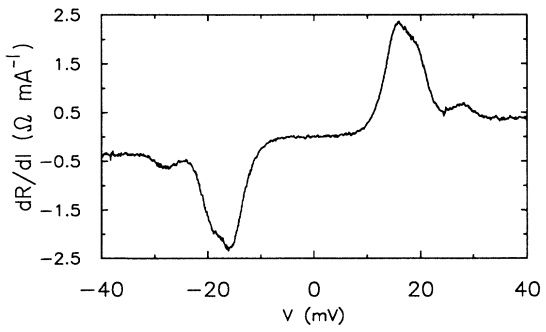


FIG. 2. Typical point-contact spectrum for a 15-Ω copper nanobridge. High-quality point-contact spectroscopy such as this, including the absence of any zero-bias anomalies, confirms that transport in these devices is predominantly ballistic.

We can infer a value for the size of the cross section of a ballistic nanobridge using Eq. (4) and the measured value of the nanobridge resistance, which is basically temperature independent from 300 to 4.2 K. Typical cross-section widths for devices showing discrete resistance fluctuations are 3–10 nm. Because the ballistic resistance is independent of the electron mean free path, depending only on sample geometry, large changes in the mean-free-path-dependent resistivity scarcely affect the estimate of the sample dimensions. Changing the resistivity to 20 times its bulk value only changes the estimated sample dimension by about 15% for a 50-Ω device. Thus the nanobridge resistance is a very dependable measurement of the diameter of the sample.

The majority of conduction electrons pass ballistically through the nanobridge from one electrode to the other, and thus these structures are strongly resistant to the effects of very high current densities. In fact, electromigration effects in these structures, which have been discussed in some detail elsewhere,[15] typically only set in at current density levels approaching or exceeding $10^9$ A/cm$^2$. In polycrystalline films at room temperatures, electromigration and thermal effects typically become significant at current densities that are several orders of magnitude lower than this. We take this as strong supporting evidence, along with the clear evidence of ballistic transport, that the typical nanobridge consists of a single-crystal dendrite that has grown through the orifice opened in the silicon nitride.

Once the nanobridges are fabricated and their ballistic nature confirmed by the measurement of high-quality point-contact spectra, the resistance noise of the device is measured as a function of temperature and bias voltage by using a battery and ballast resistor to current bias the sample, and then amplifying the noise voltage across the sample. Average fluctuation rates from $10^{-1}$–$10^4$ Hz are measured from a digitized noise signal. The actual circuit used in the direct measurement of resistance fluctuations in the nanobridges has the nanobridge as one arm of a dc bridge, with the noise voltage picked up across the arms, so that amplifiers can be dc coupled. Although this is a two-point noise measurement, comparisons with the signal observed for a four-point measurement reveal that

contact noise and contact resistance are insignificant for all but the lowest sample resistances ($R < 3\ \Omega$). In the latter cases four terminal measurements were made. The measurements discussed here are all made at bias current levels well below the point that irreversible electromigration effects commence.

## IV. $1/f$ NOISE IN NANOBRIDGES

We have studied the low-frequency noise of copper, aluminum, and palladium nanobridges with resistances ranging from 1 to 100 $\Omega$ ($c \sim 17$–$1.7$ nm). Unless the sample is sufficiently small so as to reveal the individual components of the $1/f$ noise, spectral power density measurements of the nanobridge resistance fluctuations invariably yield a $1/f^{\alpha}$ distribution where $\alpha$ ranges from 0.8 to 1.2, i.e., the samples always exhibit generic $1/f$ noise. The magnitude of the $1/f$ noise found in nanobridge measurements can be directly compared with that measured in bulk films evaporated at the same time since the noise amplitude divided by the square of the resistance, $S_R/R^2$, if it arises from the incoherent contributions of randomly distributed microscopic fluctuators, is expected to scale inversely with the sample volume. Typically this comparison is made by multiplying the measured noise power spectral density by the number of carriers $N$ and the frequency, $\gamma = NfS_R/R^2$. For our bulk copper films the room-temperature measurement of the $1/f$ magnitude yields $\gamma \sim 6\times10^{-4}$, to within a factor of 2. To compare this result to that obtained with the nanobridges, $S_R$ must be scaled relative to the diffusive part of the resistance. This is because, as is discussed in Sec. V B, one can consider the fluctuations, which are due to defect motion, to be fluctuations in the resistivity, changing the diffusive resistance of the sample. At 300 K the electron mean free path is dominated by phonon scattering, and is about 30 nm for copper films with an elastic mean free path of 180 nm. We measure an average $1/f$ noise magnitude of $fS_R/R^2 = 10^{-10}$ for the larger nanobridges, those that have a sample resistance of the order of 1 $\Omega$ and thus have a diameter of $\sim$46 nm. Because these large samples are not fully ballistic their sample size is somewhat uncertain. These measurements were done in a four-point sample holder to avoid contact resistance problems. For copper the number of electrons per cubic angstrom is $\sim$0.08, so for a sample volume of a sphere with the contact radius we find $\gamma \sim 1.6\times10^{-3}$, again to within a factor of 2. Thus to within the accuracy of the measurements (approximately a factor of 2–4) the $1/f$ noise magnitude found in nanobridges scales correctly with volume over more than five orders of magnitude.

By measuring the $1/f$ noise magnitude $S_R/R^2$ as a function of temperature we can gain some idea of the distribution of activation energies for defect motion. We actually measure $S_V/V^2$, as shown in the figures; $S_R$ and $S_V$ can be used interchangeably since for resistance noise $S_R/R^2 = S_V/V^2$. Figure 3 shows typical noise power spectral densities at 100 Hz measured as a function of temperature from 10 to 300 K for (a) copper, (b) aluminum, and (c) palladium nanobridges. In the lower-temperature region ($< 150$ K) in the case of the copper and aluminum samples, sharp peaks are often seen in $S_R$. These are due to strong Lorentzian noise sources, which, as discussed below, we attribute to a strategically placed individual defect fluctuation whose characteristic frequency is passing through the measurement frequency. At higher temperatures, where the noise amplitude is larger, such individual Lorentzians are not generally resolved and the measured noise spectrum is generic $1/f$. The figures clearly show strong differences in the distribution of defect activation energies for the three materials. In the case of aluminum samples at the lower temperatures two-level fluctuations (TLF's) are extremely rare, resulting in a noise signal too small to measure. However, beginning at about 100 K, the noise signal in aluminum rises quite rapidly with temperature. For copper nanobridges there are enough TLF's active at low temperatures to maintain a measurable signal. The noise signal gradually increases with increasing temperature, and has a distinct difference in curvature from the aluminum noise versus temperature. This suggests that, in comparison with the copper films, for the aluminum films, either the lower-energy defects are not created dur-

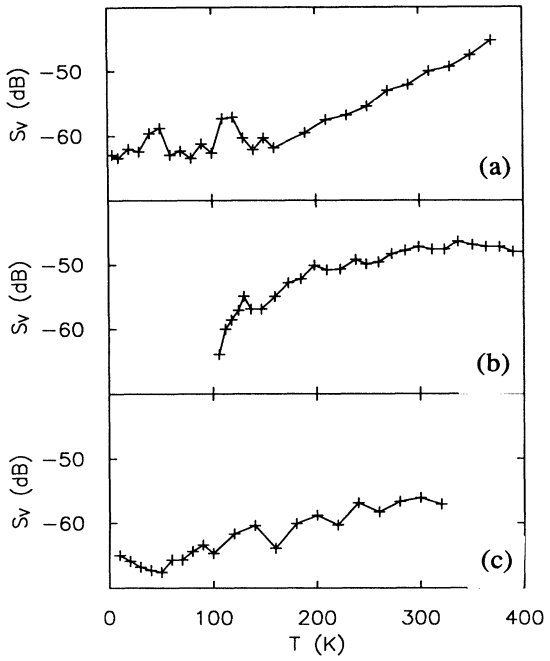


FIG. 3. Typical behavior of the noise power spectral density vs temperature for (a) copper, (b) aluminum, and (c) palladium nanobridges, reflecting the differences in activation energies for defect motion in the three materials. Below about 150 K two-level fluctuations dominate the noise signal, while at higher temperatures the noise is $1/f$. Notice that the palladium noise is fairly temperature independent, while the noise in copper and aluminum increases with temperature. Aluminum samples have far fewer active fluctuations at low temperature than either copper or palladium.

ing the film growth process or that these defects partially anneal out at room temperature in the lower-melting-point material. In the case of the palladium samples $S_R$ is almost temperature independent over the range studied. Of the three materials, palladium is of course the one with the highest melting point and thus the one with the greatest barrier for self-diffusion at room temperature. The $1/f$ noise data suggest that this results in a particularly broad distribution of defect activation energies $D(\varepsilon)$ and thus a significant density of defects with comparably low $\varepsilon$.

## V. DISCRETE RESISTANCE FLUCTUATIONS

### A. Characteristic times and energies

In the smaller nanobridges, and particularly at lower temperatures, we can observe the constituents of the $1/f$ noise directly in the real-time noise signal.[21] Such a signal contains substantially more information about the noise than does a noise power spectrum. In this section we will discuss this information in some detail. While we will present data only from copper nanobridges, the system that has been studied to the greatest extent, we see the same qualitative behavior for the individual noise components in all the metals studied to date. All the measurements that we will discuss were conducted at low enough sample voltages that the behavior of the noise was independent of bias. Electromigration effects that occur at higher biases have been discussed elsewhere; sample heating is not significant until even higher biases.

The nanobridges that are of interest here are so small that at low-temperatures ($<150$ K) there is usually no measurable sample noise other than the Johnson noise, simply because the average number of defects fluctuating in the sample volume is much less than one. But as the temperature is varied, one finds temperatures where the low-frequency noise is much higher than one would expect from the bulk $1/f$ noise measurements. Again, this reflects the fact that the $1/f$ noise has discrete constituents, so that if the sample is small enough there is an excess of noise for some energy scales and a surfeit of noise for other energy scales.

A typical example of the real-time noise signal that produces this excess low-frequency noise is shown in Fig. 4. The noise voltage switches randomly back and forth between two values. This signal is due to a change in sample resistance, for the amplitude of the fluctuation is

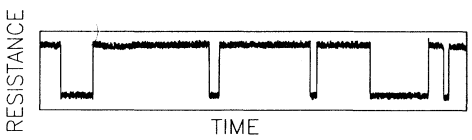


FIG. 4. Discrete resistance fluctuation characteristic of the excess low-frequency noise found in nanobridges at low temperature. Fluctuation sizes are usually $<0.1\%$ of the sample resistance; time scales vary with temperature and are thus arbitrary.

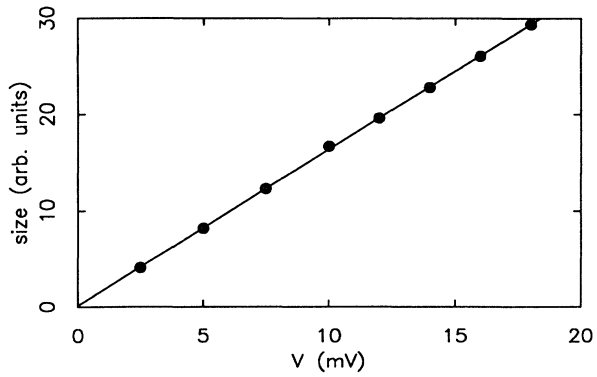


FIG. 5. The amplitude of a fluctuation is linear with applied sample bias, indicating that this noise is due to a resistance fluctuation.

linear in the bias voltage, as is shown in Fig. 5. The fluctuation amplitude is independent of temperature. A histogram of the time spent in one resistance state for a particular fluctuation is given in Fig. 6. The exponential distribution of times tells us that the fluctuation occurs with no memory as to the previous state of the system; the resistance fluctuation is Markovian. The non-Gaussian noise signal shown in Fig. 4 is thus a random two-level fluctuation of the sample resistance, and has a Lorentzian power spectrum.

The average time one of these fluctuations spends in the high or low resistance state is well described by thermally activated behavior, as shown in Fig. 7. The logarithm of the average time $\tau$ spent in one resistance state for a randomly chosen fluctuation as a function of $1/T$ is linear over four decades in time, telling us that $\tau=\tau_0 e^{\varepsilon/kT}$, where $\tau_0$ is the attempt time and $\varepsilon$ is the activation energy. A straight line fit to data such as those shown in Fig. 7 yields the first information about these fluctuations, values for $\tau_0$ and $\varepsilon$. The fluctuation pictured has $\tau_0=10^{-12.6}$ s and $\varepsilon=66$ meV.

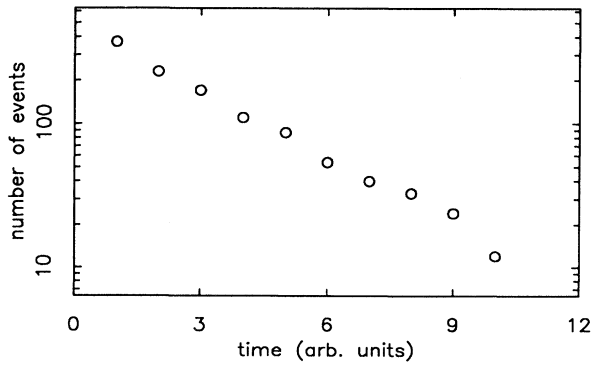


FIG. 6. Histogram of times spent in one resistance state, showing the expeonential distribution. As a result, the TLF has a Lorentzian power spectrum.

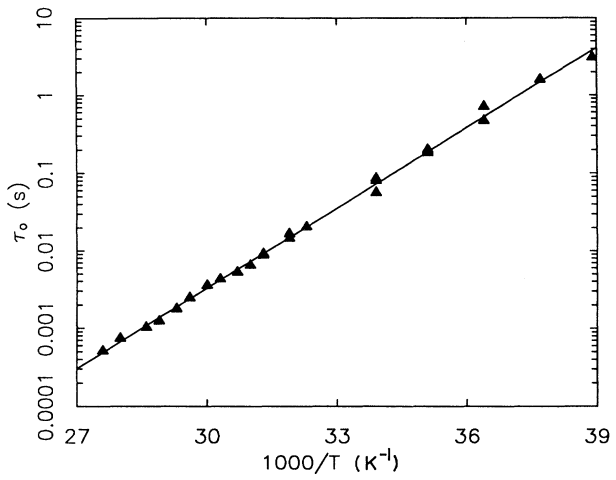


FIG. 7. Thermally activated behavior of one resistance state of a fluctuation. A fit to the data yields the attempt time and activation energy.

A summary plot of the thermally activated behavior of a collection of such fluctuators measured between 150 and 25 K is given in Fig. 8. The infinite temperature intercept gives the characteristic attempt times. Measured values range from $10^{-11}$ to $10^{-15}$ s, clustering around $10^{-13}$ s, characteristic of atomic vibration in solids. Figure 9 is a plot of the measured attempt times as a function of the temperature at which the average fluctuation time is equal to 1 s. Clearly the measured attempt time

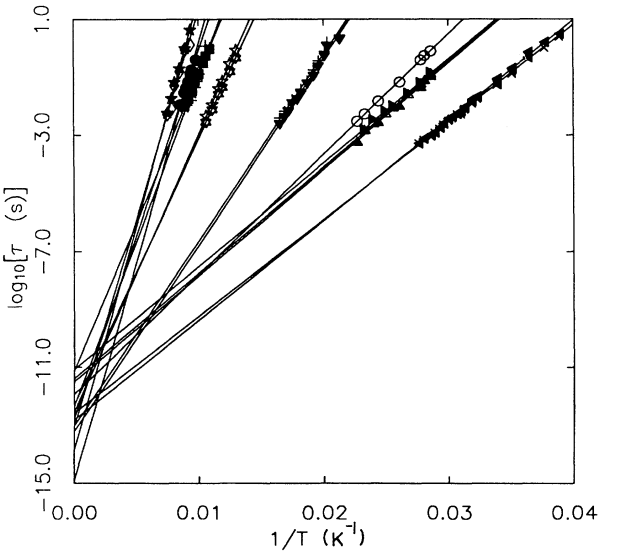


FIG. 8. Summary plot of thermally activated behavior for many different defect fluctuations. Attempt times range from $10^{-11}$ to $10^{-15}$ s, as shown by the $y$ intercept. Activation energies come from the slopes of the lines, and tend to increase with increasing temperature.

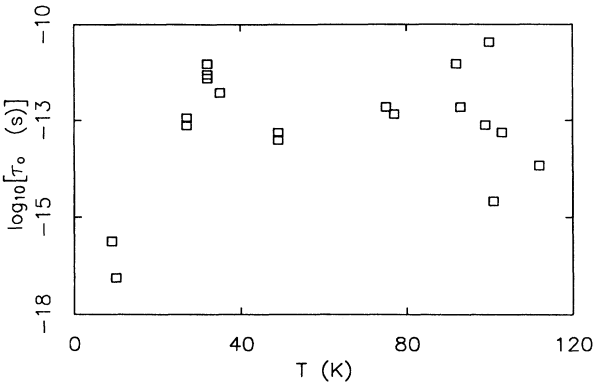


FIG. 9. Measured attempt times for many different defects as a function of the temperature at which the fluctuation was studied. No correlation with temperature is observed.

shows no correlation with temperature. The slopes of the lines in Fig. 8 reflect the activation energies, with measured values ranging from 30 to 300 meV. (Defect fluctuations with about 10-meV activation energy have been seen, but an exact value for the activation energy has not been measured for this type of fluctuation, which is very rare in the crystalline copper nanobridges.) Note that at these temperatures ($T < 150$ K) we are studying only the low-energy tail of the distribution of defect fluctuations deduced by a Dutta and Horn analysis[13] of the $1/f$ noise in larger nanobridges. Indeed, $\tau_0$ fixes the activation energy that will cause the noise to fall within the experimental bandwidth for a given temperature. In general, the higher the temperature range in which an active state is found, the higher the value of the two activation energies measured; as can be seen in the figure, the size of the slope is larger for the fluctuations found at higher temperatures. As seen in Fig. 10, the activation energy roughly obeys $\varepsilon = 2.6 T_{1s}(\mathrm{K})$ meV. This implies a typical attempt time of $10^{-12.9}$ s and that the actual distribution of $\tau_0$ about this value is comparatively narrow. Thus a

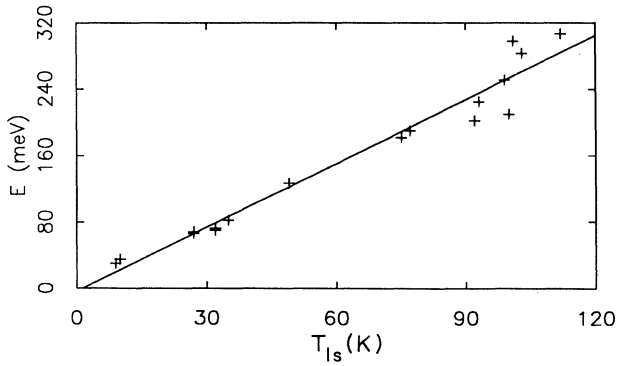


FIG. 10. Measured activation energies for many different defects, as a function of the temperature at which a fluctuation was studied. A fit to the data yields $\varepsilon = 2.6 T_{1s}(\mathrm{K})$ meV.

fairly good estimate of the activation energy can be made with the observation of a TLF at a single temperature. We find, therefore, that the direct microscopic measurements of defect fluctuations does substantiate the simplifying assumption by Dutta and Horn[13] of a constant attempt time. This information is particularly useful for $T > 150$ K, where stable TLF's do not exist.

We note that this discrete resistance noise was apparently observed in bulk metal point contacts by Yanson, Akimenko, and Verkin several years ago,[22] although the data were not interpreted in this fashion. Yanson and co-workers observed peaks as a function of sample bias in the noise spectral density measured at a fixed frequency at low temperatures. Were we to measure the nanobridge noise in this fashion, that is exactly what we would observe. This is because the fluctuation rate for the TLF's increases with increasing sample voltage at moderate voltages. These TLF's have a Lorentzian noise spectrum, $S_R/R^2=\tau/(1+\omega^2\tau^2)$, with a knee frequency given by the sum of the characteristic frequencies in each of the two states, $\tau^{-1}=\tau_1^{-1}+\tau_2^{-1}$ and a low-frequency amplitude for the Lorentzian that decreases as the inverse of the knee frequency $\tau^{-1}$. An observation conducted at a fixed frequency measures an increasing noise spectral density as $\tau^{-1}$ passes through the measurement window, and then a decreasing spectral density as $\tau^{-1}$ increases still further. This independent observation of TLF noise by Yanson, Akimenko, and Verkin in bulk metal point contacts larger than those used in our experiments shows the general nature of the phenomena being studied here.

### B. Amplitude of the fluctuations

The size of the resistance fluctuations can be used to estimate the size of the change in scattering cross section. Because of the three-dimensional geometry of a point contact, the current density in a nanobridge is highest in the narrowest part of the device, falling off into the electrodes. This means that a scatterer has a greater impact on the sample resistance the closer it is to the narrowest part of the device. Assuming that the largest fluctuators observed in any given sample are due to scatterers in the center of that device, the change in the scattering cross section $\Delta\sigma$ can be estimated. There are two possible approaches to this estimate, based on the two terms that together approximate the resistance of a point contact.

The first approach is to say that $\Delta\sigma$ changes the cross-sectional area of the device, and thus affects the ballistic resistance. Then using Eq. (3),

$$R+\Delta R=\frac{4\rho\lambda}{3(\pi c^2-\Delta\sigma)} , \tag{10}$$

and for $\Delta\sigma \ll \pi c^2$ we find that the measured percentage resistance change is roughly equal to the percentage area change

$$\frac{\Delta R}{R}\sim\frac{\Delta\sigma}{\pi c^2} . \tag{11}$$

The second approach is to say that $\Delta\sigma$ changes the resistivity in the nanobridge region, and thus affects the diffusive resistance [Eq. (2)]. The resistivity is related to the cross sections of all the scatterers by the relation

$$\rho\approx\frac{k}{\lambda}\approx\frac{k}{\mathcal{V}}\sum_i\sigma_i , \tag{12}$$

where $k$ is a constant, so that the change in resistivity is given by

$$\Delta\rho\approx\frac{k}{\mathcal{V}}\Delta\sigma\approx\frac{\rho\lambda}{\mathcal{V}}\Delta\sigma , \tag{13}$$

and the change in resistance relative to the diffusive resistance is

$$\frac{\Delta R}{R_D}=\frac{\Delta\rho}{\rho}\approx\frac{\lambda}{\mathcal{V}}\Delta\sigma . \tag{14}$$

What is measured is the change in resistance relative to the total resistance, which for devices in the ballistic transport regime is roughly the same as the change in resistance relative to the ballistic resistance. Thus we find

$$\frac{\Delta R}{R}\approx\frac{9\pi}{32}\frac{\Delta\sigma}{\pi c^2} , \tag{15}$$

which is essentially the same as Eq. (11).

Figure 11 shows a plot of the percent resistance change for the largest fluctuations observed in any given sample as a function of the nanobridge resistance. Although there is considerable scatter to the data, the straight-line fit shows the slope $\Delta R/R \propto R$ expected from Eq. (11). Note that this result provides further evidence that the nanobridges are in the ballistic transport regime; in the diffusive regime we expect $\Delta R/R \propto R^3$. The measured values for $\Delta\sigma$ are plotted in Fig. 12 as a function of sample resistance in order to show that the $\Delta\sigma$ values deduced from Eq. (11) are indeed independent of sample resistance. Measured values of $\Delta\sigma$ range from 0.28 to 3.6 Å$^2$, on the order of atomic dimensions. This is consistent

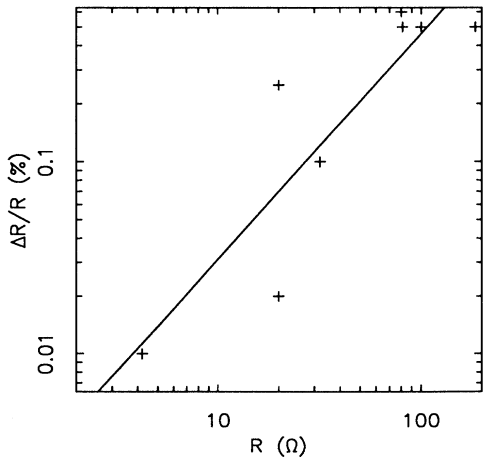


FIG 11. Percent resistance change vs sample resistance for the largest fluctuation every observed in a given sample. A slope of 1 is expected for ballistic point contacts.

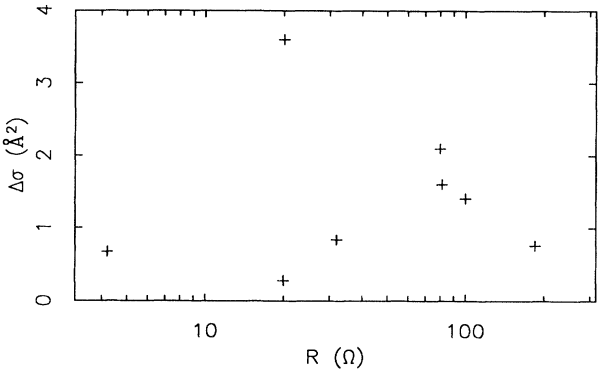


FIG. 12. Calculated scattering-cross-section change vs resistance for the largest fluctuation ever observed in a given sample. Values are atomic-sized over two decades of sample resistance.

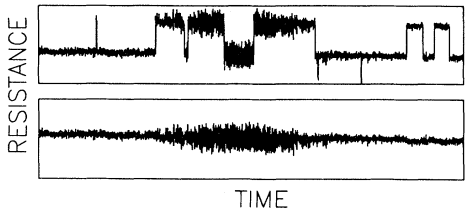


FIG. 13. Noise signal characteristic of a defect diffusing through the nanobridge, as measured, superposed on an ordinary TLF (top), and with the superposed TLF signal subtracted out (bottom). Initially background noise dominates, then the noise signal gradually increases as the defect enters the device, reaches a maximum, and then decreases as the defect leaves the device.

with estimates made for atomic-scale defect reorientation in clean metals, although as discussed below these defect fluctuations are not due to the reversible reorientation of simple defects. Smaller cross-section changes may exist, but are indistinguishable from larger changes of scatterers far from the center of the device, due to the three-dimensional nature of the device.

Note that we do not see anomalously large values for $\Delta\sigma$ as reported recently by Giordano and Schuler.[23] We previously reported a larger possible range of $\Delta\sigma$,[21] reflecting a (then) larger uncertainty as to the cleanliness and therefore the dimensions of our samples. However, as discussed in Sec. III, subsequent data taken on nanobridges known to have a significant diffusive contribution to the resistance show universal conductance fluctuation effects. As we never see these effects in the clean nanobridges used for noise studies discussed here, we can now place a much more stringent constraint on the sample dimensions.

The atomic-scale change in the scattering cross-section, together with the measured attempt times, shows that this discrete resistance noise is due to defects fluctuating reversibly between metastable configurations. These TLF's, which are the dominant source of low-frequency noise in the nanobridges, are not due to defects diffusing through the sample, for they show stable fluctuation amplitudes over days of observation. Only on rare occasions is noise attributable to the diffusion of a defect through the system observed; an example of such a noise signal is presented below.

### C. Diffusion noise

A very rare type of noise is shown in Fig. 13, that due to a defect diffusing through the nanobridge region at 20 K, superimposed on a TLF signal. The TLF signal has been subtracted for clarity in the lower noise snapshot in Fig. 13. Because the current density is not uniform throughout the nanobridge region, the effect a scatterer has on the total resistance depends on where in the device it is located. Thus the noise signal shown in Fig. 13 gradually increases as the defect enters the device region, reaches a maximum as it passes through the center, and then gradually decreases as the scatterer leaves the device region. Figure 14 is a time expansion of the signal in Fig. 13, showing that resistance changes occur roughly 100 times a second. Although this signal was filtered at high frequency and thus is not sharp, each change in the sample resistance presumably represents a jump of the defect by about one lattice spacing.

It is unlikely that this defect was merely a flaw in the crystalline structure of the copper, such as a vacancy, because such a structural defect, if mobile, would readily combine with other structural defects and therefore disappear. Thus this diffusion noise signal is likely due to an impurity. However, the impurity moved through the sample very rapidly—the diffusion constant is on the order of $10^{-14}$ cm$^2$/s at 20 K. At low temperature the most mobile impurity species is H. But even if this defect were hydrogen, it is likely that the high field ($\sim 10^4$ V/cm) and high current density ($\sim 10^8$ A/cm$^2$) found in nanobridges at low biases (10 mV) served to accelerate the diffusion process, causing the defect to electromigrate.

The size of this resistance fluctuation, on the order of a

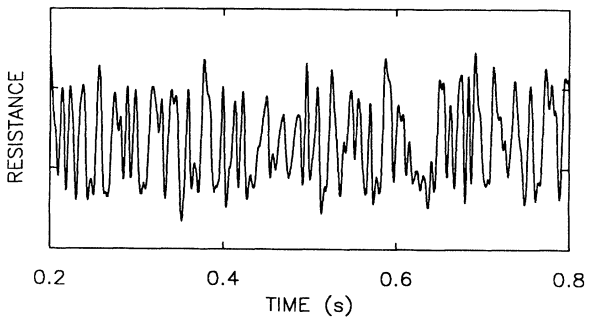


FIG. 14. Time expansion of the diffusion noise signal. Each resistance change is presumably due to a single atomic hop of the diffusing defect.

hundredth of a percent of the nanobridge resistance at its maximum, is not particularly surprising. However, it is quite strange that the resistance fluctuations occur both above *and* below the average sample resistance. As discussed in Sec. III, these samples are not in the universal conductance fluctuation regime, so the most likely explanation for resistance fluctuations below the average resistance due to the diffusing defect is that the impurity is deforming the lattice locally, thereby reducing the scattering cross section of some of the nearby structural defects. Indeed, the diffusing impurity could effectively remove another defect if it were to occupy space along the surface or within a vacancy cluster.

## VI. DEFECT INTERACTIONS

### A. Ubiquity of defect interactions

The stability and two-level character of the defect fluctuations gives an important insight into the microscopic nature of the fluctuating defect. It cannot be a simple point defect, such as a vacancy or impurity atom, embedded in an otherwise perfect lattice as this would not result in a stable two-level resistance fluctuation. Instead the defect must at least have a dipolar component and the dipole must be sufficiently strongly bound to a particular point in the lattice so that while its orientation can change, the center of mass of the defect cannot diffuse, at least not during the measurement period. This suggests that interactions between defects are important for producing stable two-level fluctuations.

Figure 15 shows two TLF's fluctuating at the same time, apparently independent of each other. This apparent independence of defect fluctuations in the metal nanobridges is, however, not the general rule. Quite frequently, the defect fluctuations interact, with the reconfiguration of one defect clearly affecting the characteristic times of another defect fluctuation. Indeed, when careful measurements of defect fluctuation times are made, it is rare to find simultaneous fluctuations that are independent. An example of interacting defect noise is shown in Fig. 16; when the slow two-level resistance fluctuation is in its high resistance state, there is a very rapid fluctuation that apparently disappears when the slow fluctuation is in its low resistance state. Often the strength of the interaction is not quite so strong. Figure 17 shows the characteristic fluctuation behavior of one defect (a) before and (b) after another defect has reconfigured. As an example we have analyzed the changes that occur in the activation energies and fluctuation attempt rates that occur in one fluctuation as result

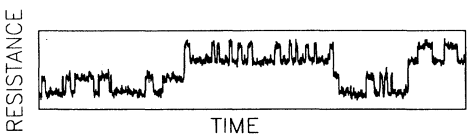


FIG. 15. Apparently noninteracting defect fluctuations.

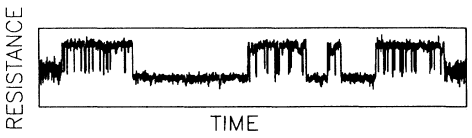


FIG. 16. Strongly interacting defect fluctuations. Note that when the slowly reconfiguring defect is in its high resistance state there is a rapidly reconfiguring defect that leaves the experimental bandwidth when the slowly reconfiguring defect is in its low resistance state.

of the change of state of another, slower fluctuation. Both fluctuations stay well within the four decades of measurement bandwidth during the study. We found that the biggest change was that one of the two activation energies of the modulated defect fluctuation went from 72 to 82 meV, but the other activation energy and the attempt rates changed as well. Frequently, as in Fig. 16, the fluctuation moves completely out of the experimental bandwidth, and, assuming that the change in activation energy dominates, we can only place a lower bound on the change in activation energy $\Delta\varepsilon$ due to the interaction. Using the relation found earlier $\varepsilon = 2.6 T_{1s}(\mathrm{K})$ meV, we find that if a TLF becomes 1000 times faster, then $\Delta\varepsilon/\varepsilon > 0.3$. Clearly the detailed potential governing the behavior of one defect is being modulated by the reconfiguration of another defect.

Most defect interactions that have been observed are of the type just described where the interaction modifies the dynamics of one fluctuation but does not measurably change the amplitude of the resistance change. An example of a much rarer type of interaction between defects is shown in Fig. 18, where the reconfiguration of one defect modifies the scattering-cross-section change of another defect fluctuation. Here notice that when the slowly reconfiguring defect is in its low resistance state the rapidly reconfiguring defect has a larger resistance change than when the slowly reconfiguring defect is in its high resistance state. Such an interaction indicates that the total scattering cross section is not just the sum of the scattering cross sections of the two defects. If these nanobridges were in the universal conductance fluctuation regime, such amplitude modulation between in-

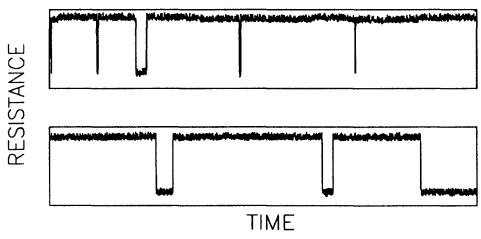


FIG. 17. Snapshots of a TLF before and after another defect has reconfigured. This interaction is much weaker than that shown in Fig. 16.

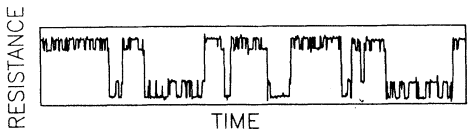


FIG. 18. Amplitude modulation for interacting TLF's. Note that the smaller TLF has a larger resistance change when the slowly reconfiguring defect is in its low resistance state than when the slowly reconfiguring defect is in its high resistance state.

teracting defects would be common and could extend over considerable distances. However, the nanobridge samples of concern here are not in the universal conductance fluctuation regime, and this amplitude modulation is quite rare. For local interference effects to occur, the fluctuating defects must be within a lattice spacing or so of each other to display amplitude modulation.[9] Apparently this is uncommon to these comparatively clean metal nanobridges.

In the copper nanobridges stable interactions between defect fluctuations can only be examined at temperatures less than $\sim 150$ K. As temperature is raised we find that, as expected, more and more fluctuations become active in the experimental bandwidth. Interactions between defects become more common, and at a temperature above about 150 K it is no longer possible to find a stable TLF. In the larger nanobridges $R < 50\ \Omega$ ($c > 2.4$ nm), at this temperature the number of active defects is sufficiently high that individual two-level fluctuators cannot be resolved, and only the resulting $1/f$ noise spectrum can be examined. But in the smallest nanobridges considerably more insight into the nature and effect of the defect interactions can be gained in the higher-temperature regime. Above about 150 K interactions between defects dominate the fluctuation dynamics, and although the sample is sufficiently small that the noise signal at any given instant is still composed of distinguishable discrete resistance fluctuations, the magnitude, characteristic time, and number of defects active in the experimental bandwidth fluctuate in time. Four snapshots illustrating this fluctuating noise behavior in a 90-$\Omega$ copper nanobridge at 300 K are shown in Fig. 19. Sometimes a small TLF is active, sometimes a large TLF is active, and sometimes there are apparently no TLF's active within the experimental bandwidth. It appears quite inappropriate to ascribe such a noise signal to independent defects.

The real-time noise found at 300 K, such as is shown in Fig. 19, when analyzed over a sufficient time period has a smooth $1/f$ spectrum, as shown in Fig. 20. Thus we see that the interactions between defects cause the system to sample all times, even when there is on average only one defect active at a given time within the measurement bandwidth in the sample volume. This is a very different way of obtaining a $1/f$ spectrum than the standard model of a collection of randomly distributed, independent Lorentzian noise sources presented in Sec. II. The $1/f$ power spectrum of course contains no hint of the rich

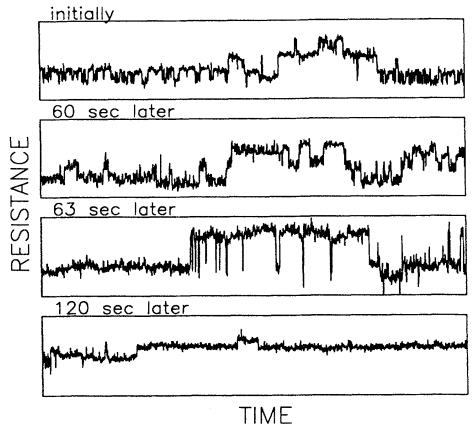


FIG. 19. Fluctuating noise behavior in a 90-$\Omega$ copper nanobridge at 300 K characteristic of the high-temperature noise seen in the smaller nanobridges. Independent TLF's are never seen above about 150 K, telling us that all the active defects are interacting strongly with other active defects.

complexity found in the microscopic system. We clearly see that there are at least two different ways of producing a $1/f$ spectrum, which can only be distinguished by studying the noise at the microscopic level.

We should note here, however, that while the interactions do lead to considerable complexity in the real-time

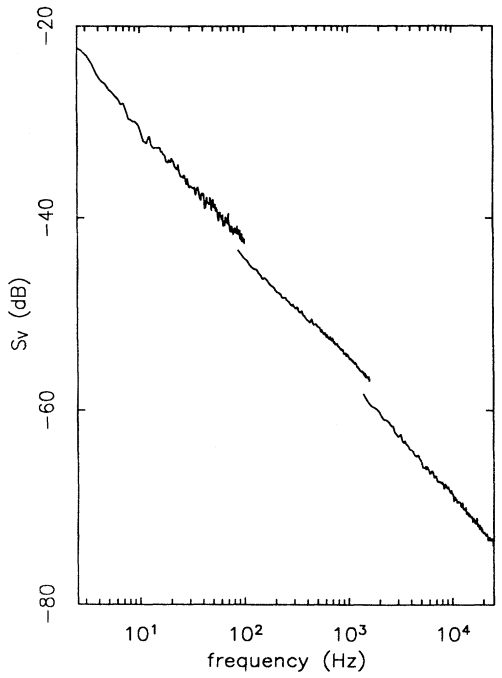


FIG. 20. $1/f$ behavior of a fluctuating noise signal such as that found in Fig. 19, showing that the noise samples all time scales. The breaks in the data result because the three different bandwidths are measured at separate times.

noise behavior of small structures, they do not have a dramatic effect on the magnitude of the $1/f$ noise. This can be understood readily, for the interactions can be negative as well as positive. That is, a fluctuation to a higher resistance state can influence another defect to prefer its high resistance state, thereby increasing the root-mean-square noise above that due to independent defects, but it is also possible for a fluctuation of one defect to its high resistance state to influence another defect to prefer its low resistance state, which leads to a smaller root-mean-square noise signal than for independent defect fluctuations. In practice we observe both kinds of interactions, and have no reason to expect one type to dominate over the other.

### B. Size dependence of noise and interactions

In drawing general conclusions concerning the microscopic nature of $1/f$ noise in metals from the behavior of defect fluctuations in metal nanobridges, it is essential of course to ensure that what is being studied in the nanobridges is in fact the same phenomenon that is seen as $1/f$ noise in bulk films. The fact that the $1/f$ noise measured at room temperature in larger nanobridges scales very closely with that measured in bulk films deposited in the same manner demonstrates this direct connection, as does the independent observation of TLF's by Yanson, Akimenko, and Verkin in bulk metal point contacts.[22] However, we should note that the noise level seen at the higher temperatures in the smallest nanobridges is systematically higher than that expected by scaling from the bulk and larger nanobridge results. This is seen in Fig. 21, where we show $fS_R/R^2$ as a function of $R$ for many copper nanobridges at 300 K. As discussed in Sec. V B, we expect an individual fluctuation to scale as $\Delta R/R \sim R$. Assuming independent defect fluctuations

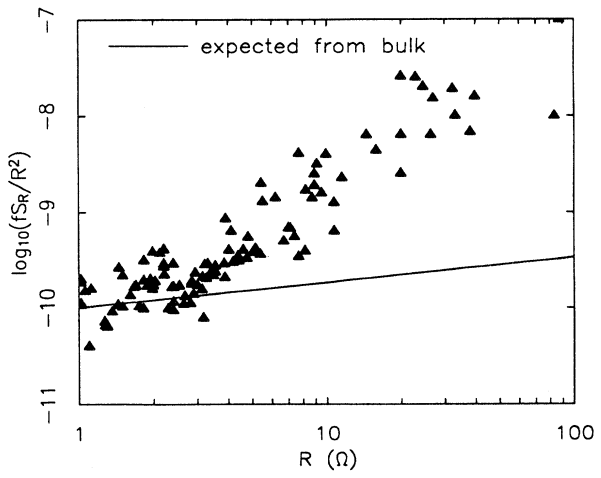


FIG. 21. Noise power spectral density scaled by frequency and $R^{-2}$ for many samples of different resistance. At small resistance ("large" devices) the noise power observed is consistent with that found in the bulk. At large resistance (small devices) the noise increases more rapidly than expected.

$$\frac{S_R}{R^2} \propto N\frac{\langle(\delta R)^2\rangle}{R^2} \propto NR^2 , \tag{16}$$

where $N$ is the number of noise sources. For a constant density of noise sources we expect $N=c^3$ so that the noise should then scale as $S_R/R^2=R^{0.5}$. Generally what we observe is $S_R/R^2=R^{1.5}$. This implies that there are more defects active in the smaller samples than we would expect from observations of larger samples. Note this does not mean we must necessarily have a higher total density of defects present in the smaller samples, just a higher density of *active* defects.

The most likely explanation for the excess number of active fluctuators stems from the fact that the extremely small radius of curvature of the nanobridges means the surface tension of the structure significantly affects its behavior. The strength of this surface tension force becomes apparent when copper nanobridges are annealed for even 1 min at such moderate temperatures at 300 °C. Under such conditions the constriction pulls itself apart, resulting in an open circuit where once there was continuous metal. The effect of a very small radius of curvature is to effectively lower the melting temperature, and hence the activation energies for atomic motion within the nanobridge below that of the bulk material. (If the melting point is low enough in the constriction region, we might expect defects to be created and destroyed in significant numbers at 300 K. However, the stability of the small samples over many weeks at 300 K suggests that at this temperature the energy for point-defect formation and diffusion has not yet been lowered sufficiently so that the structure as a whole is unstable or that the structural defects are freely mobile.)

Dutta and Horn, in their study of the $1/f$ noise of bulk copper films,[13] found that the $1/f$ noise magnitude in copper increases with increasing temperature to a maximum at about 500 K. If the melting temperature and hence the activation energies for atomic motion are lower the smaller the nanobridge is, we would expect this $1/f$ noise peak to also occur at a lower temperature the smaller the nanobridge. Indeed, such a peak in the $1/f$ noise at 350 K has been observed as illustrated in Fig. 22 for a 7-Ω ($c \sim 6.4$ nm) nanobridge. However, in most of the nanobridges studied the noise magnitude just keeps increasing as the temperature is raised, until finally the device pulls apart. The melting of the device obscures the measurement of the peak in defect fluctuation activity.

While a decrease in the effective melting temperature of the smaller nanobridges would appear to readily explain the greater than expected noise level, we also expect that a somewhat higher density of defects would form locally in the constriction region during deposition as a result of accommodating the greater strain due to the high radius of curvature. If we make the limiting assumption that all the excess fluctuators are due to additional structural defects, the local elastic-scattering length in the smallest samples would then be about 60 nm, not 180 nm as it is in the bulk film. But even then the nanobridge would still be in the ballistic transport regime, as is independently confirmed by the excellent point-contact electron-phonon spectra obtained with the smallest nano-

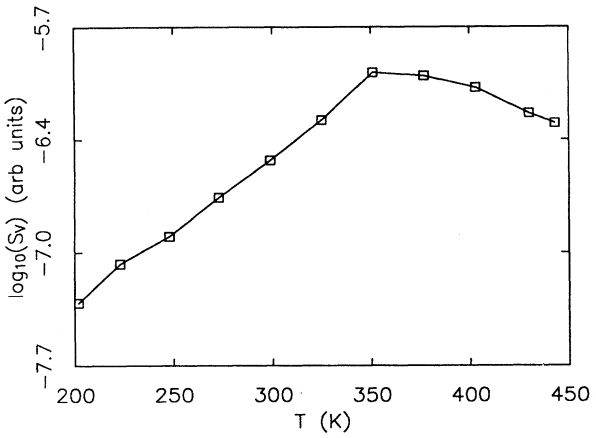


FIG. 22. Peak in $1/f$ noise as a fucntion of temperature for a copper nanobridge. This behavior is consistent with the Dutta-Horn results if relevant temperature scales are lower in the nanobridges due to the tiny radius of curvature. Typically the nanobridge pulls itself apart before such a noise peak is observed.

bridges, and the defect density would be comparable to that found in the cleaner films whose $1/f$ noise has been studied in the literature. It is quite likely, of course, that the effects both of accommodating strain and of a lowered effective melting temperature are conspiring to increase the number of defect fluctuations evident in the smallest nanobridges.

Regardless of the exact details of the explanation for the greater than expected noise level in the smaller nanobridges, we find that the implications of the complex interactions between defects that are seen directly in the higher-temperature noise signal of the high resistance nanobridges are quite general. While there may be a quantitative change in the activation energy distribution, or in the density, of the defects that result in $1/f$ noise, the strong interactions between such defects remain present in the larger nanobridges and thus, by extension, in the bulk film. Even if the smallest nanobridges have an elastic mean free path locally of 60 nm, they are still as clean or cleaner than many bulk films used for studying $1/f$ noise in "clean" metals. Indeed, as discussed in the following section, the observed density of active defects in the smallest nanobridges contributing to the $1/f$ noise is still smaller than or equal to the total defect density found in our bulk films. Thus the defects in our bulk films are closely spaced enough to show the strong interactions we observe in the small nanobridges. The apparently stable condition of the active two-level fluctuators may well persist to higher temperatures in the larger nanobridges and in the bulk film than is the case for the smaller nanobridges, but this does not fundamentally alter the fact that it is the interactions between defects that generally determine the activation energies of individual TLF's that result in the overall $1/f$ noise.

## VII. DISCUSSION

The observation of discrete, at least quasistable, two-level fluctuations as the dominant source of low-frequency noise in the as-deposited metal nanobridges, and the close scaling of the overall $1/f$ level with that measured in bulk films fabricated in the same manner, strongly suggests that such fluctuations are the general origin of the ubiquitous $1/f$ noise found in metal films. As discussed above, an elastic dipole appears to be the simplest type of structural defect that can result in stable two-level resistance fluctuations. The scale of the directly measured changes in the scattering cross section, $\Delta\sigma \sim 1$ Å$^2$, in these fluctuations is also very consistent with the activated rotation of dipoles between metastable orientations, as is the measured fluctuation attempt rate. Thus a very simple model of the defects involved in the $1/f$ noise in a metal would be a random distribution of atomic-scale elastic dipoles. If we assume further that all electron scattering in the metal arises from such dipoles, then an elastic mean free path $\lambda_e = 180$ nm and a total dipolar scattering cross section $\sigma$ of 2 Å$^2$ gives an average dipole-dipole spacing $r = 1.5$ nm. If $\lambda_e = 60$ nm, which is the lower estimate for the smaller copper nanobridges, then we have $r = 1.0$ nm. We acknowledge that this model of randomly distributed dipoles, while chosen for its tractability, is undoubtedly overly simplistic. However, we also note that this model is consistent with the apparent requirement that, in general, the fluctuating defects must be several angstroms apart or the amplitude modulation of the two-level resistance fluctuation would be much more common than is observed. We will use this model below to estimate the expected interaction energy between defects.

Given that we know the characteristic fluctuation amplitude for the constituents of the $1/f$ noise, we can also estimate the percentage of all the defects in the sample that are participating in the low-frequency fluctuations in the context of this dipole defect model. Using the standard model for $1/f$ noise, a flat or slowly varying distribution of characteristic times indicates that $fS_R$ is about $0.7\langle(\Delta R)^2\rangle D$, where $D$ is the number of defects active per frequency decade. If we assume that the average fluctuation size is $\frac{1}{5}$ of the largest observed in a given size sample (as appears to be true experimentally), and that one of every three fluctuations does not produce a resistance fluctuation because it occurs parallel to the direction of current flow, then we have measured values of all of the parameters needed to estimate $D$ from the observed $1/f$ noise amplitude. From Fig. 21, we find that $fS_R/R^2 \sim 10^{-7}$ for a 100-Ω device and $\sim 3\times 10^{-10}$ for a 3-Ω device. Assuming a uniform spatial distribution of the defects that are fluctuating at 300 K in the four decades of measurement bandwidth for a 100-Ω ($c \approx 1.7$ nm) nanobridge, we find that the volume per such defect is $\sim 2.5\times 10^4$ Å$^3$. For a 3-Ω ($c \approx 9.8$ nm) nanobridge, we find that the volume per fluctuating defect is $\sim 5\times 10^5$ Å$^3$, indicating a factor of 20 lower density of active defects in the larger nanobridges. The result is that for a 3-Ω nanobridge, and for a mean free path $\lambda_e = 180$ nm, $\sim 0.5\%$ of the dipolar defects are actively fluctuating in the measurement bandwidth at 300 K. For a 100-Ω nanobridge, $\sim 10\%$ of the defects are active, if we assume again that $\lambda_e = 180$ nm. If we assume that $\lambda_e = 60$ nm, then we find the same percent of defects active as in the

larger device.

Of course, dipoles whose mean fluctuation rates are outside the measurement bandwidth should also be considered active if they have a significant probability of undergoing at least one change during experimental time scales. We can very roughly estimate the total percentage of such active defects by assuming that $fS_R$ is constant over 16 decades of frequency, extending from $10^{13}$ to $10^{-3}$ Hz, where the lower-frequency limit is taken so as to be approximately equal to the inverse time of a typical noise measurement. This estimate thus raises the percentage of defects that can be considered active by a factor of 4. Given the experimental observation that $fS_R$ increases with $T$, this approach clearly underestimates the number of defects with the higher activation energies that are active and overestimates the number of active defects with the lower activation energies. A safe *overestimate* of the number of defects that can be considered active at a given $T$ is to measure $fS_R$ and hence determine $D$ for the measurement bandwidth at a temperature that is $\sim 25\%$ higher and then use this $D$ to estimate the number of defects fluctuating over the entire "active bandwidth" at $T$, as long as one is measuring below the peak in the noise found by Dutta and Horn.[13] From temperature-dependent $fS_R$ data obtained with a typical copper nanobridge, this approach suggests that the total number of defects in a copper nanobridge that can fluctuate during a measurement period is no greater than 20 times the number that contribute to the $1/f$ noise measured over the experimental bandwidth at 300 K. Thus of order 10% or less of all the electrical defects in the larger nanobridges can be considered active at 300 K, while in the smallest nanobridges 5–100 % of the defects (depending on the value of $\lambda_e$ for the nanobridge) may be fluctuating at least once during a measurement. Again this difference is largely attributed to the greater stress on the smaller nanobridges due to their very small radius of curvature. It is interesting to note from such an analysis that when a nanobridge sample begins to approach the point where either $S_R$ peaks or the sample begins to pull apart, a majority of the electrical defects have begun to participate in producing the $1/f$ noise.

While the density of fluctuating defects that is necessary to account for the $1/f$ noise is consistent with a randomly distributed dipole defect model, the interactions between TLF's that were described in the preceding section demonstrate that a simple picture of a collection of "independent" fluctuating dipolar defects combining to yield $1/f$ noise is a very poor approximation to what is a richly complex situation of interacting structural defects. Indeed, since the attempt rate for the constituent Lorentzian noise sources is found to be fairly narrowly distributed about $10^{13}$ Hz, strong defect-defect interactions must clearly be an integral part of the generation of $1/f$ noise, if ionic motion is involved. This is simply because the activation energies for defect motion in an otherwise perfect crystal are discrete, with characteristic activation energies for atomic motion $\varepsilon \geq 1$ eV. But $1/f$ noise requires a broad distribution of activation energies, extending well below this characteristic energy scale, with the breadth of the distribution depending on how low in temperature the system continues to exhibit a significant $1/f$ noise signal. For the metal nanobridges we find that fluctuations occur at temperatures as low as 4.2 K. Although such fluctuations are extremely rare, their presence requires some defects to have activation energies for reversible reorientations that are $\sim 0.01$ eV. An assembly of randomly, but fairly strongly, interacting defects is the most straightforward way, perhaps the only way, of establishing such a situation, and is fully consistent with the direct observation of the complex noise behavior of the metal nanobridges.

Thus, insofar as the atomic defects that are responsible for $1/f$ noise are concerned, we must conclude that there is no such thing as an independent defect even in crystalline films with elastic-scattering lengths of 200 nm. Of course a metal film certainly can have atomic defects whose behavior is effectively independent of that of other neighboring defects. But, at least if these are simple point defects, they will not have the required low activation energies and will not contribute stable two-level fluctuations to the $1/f$ noise. Instead the defects involved in $1/f$ noise are so strongly interacting that they must be considered as an interconnected defect system or "defect glass" which allows some elements of the interconnected defect system to fluctuate in a very complex potential. This potential is formed by the random defect interactions. The effective "melting point" of this defect glass can then be defined as that point when a sufficient density of defect fluctuations have become active such that the defect potential is no longer stable, apart from reversible fluctuations, but instead begins to constantly evolve in time. For the case of the smaller copper nanobridges this defect-glass melting point is approximately 150 K for our experimental bandwidth. For the larger nanobridges, which may have a somewhat lower defect density and thus a somewhat weaker average defect interaction strength, the temperature region in which the TLF's are more or less stable may extend somewhat higher. As discussed previously, the larger sample size obscures the direct observation of the melting point. But since it is apparent that the defect interactions still determine the defect potential in this case, a general melting of the defect glass will certainly occur in some temperature region that is well below the melting point of the lattice.

An important result of our ability to directly observe the interactions between individual defect fluctuations is that we can estimate the range of the interaction mechanism. At low temperatures, $T \leq 150$ K, where TLF's can be resolved in the larger nanobridges, interactions typically change the average fluctuation rate by more than a factor of 10, indicating a fractional interaction energy $\Delta\varepsilon/\varepsilon \geq 0.1$ [as before we have eliminated $T$ by using the measured relation that on average $\varepsilon = 2.6 T_{1s}(\mathrm{K})$ meV]. If the fluctuating defects are randomly distributed dipoles, then the average separation between the defects is at least 1.0–1.5 nm. Of course, as we have noted, only a fraction of scattering centers in a metal are participating in the low-frequency two-level resistance fluctuations at low temperature and thus the average distance over which the interaction energy is $\sim 30$ meV must be considerably greater than 1.5 nm. A different estimate of the interac-

tion range that does not depend so strongly on the assumption of a random distribution of defects can be obtained from the measurements on the smallest nanobridges at temperatures above their defect-glass melting point. For example, in a 90-Ω copper nanobridge at 300 K there is on average one defect fluctuation active in our experimental bandwidth, and interactions are constantly changing the nature of the noise. This indicates that all the active defects within the nanobridge region are strongly interacting and implies an interaction length of at least the sample dimensions, 1.7 nm. In these same samples we see that interactions changing the fluctuation rate by at least a factor of 10 are the norm, implying a $\Delta\varepsilon$ of at least 60 meV for this interaction length.

The most likely mechanism for the interaction between defect elements is through the lattice elastic strain field. For dipolar defects we can estimate the size of the interaction energy $\Delta\varepsilon$ that we would expect from linear elasticity theory. Keep in mind, of course, that we expect the defect structure in the actual metal to be much more complicated than that of isolated dipoles. From Grannan, Randeria, and Sethna,[24] we have that $\Delta\varepsilon$ for a stable relative orientation of two elastic dipoles is

$$\Delta\varepsilon = A(E_1+E_2)\frac{Q^2}{z^3} , \tag{17}$$

where $z$ is the dipole separation,

$$\begin{aligned} E_1 = 2(&\tfrac{4}{3} - 2\cos^2\alpha\sin^2\theta - 2\sin^2\alpha\cos^2\theta \\ &- 2\sin^2\alpha\sin^2\theta\cos^2\phi \\ &+ 2\cos\alpha\sin\alpha\cos\theta\sin\theta\cos\phi) , \end{aligned} \tag{18}$$

and

$$\begin{aligned} E_2 = 2B(&\tfrac{8}{3} + 5\sin^2\alpha\sin^2\theta - 4\sin^2\alpha - 4\sin^2\theta \\ &+ 2\sin^2\alpha\sin^2\theta\cos^2\phi \\ &- 8\cos\alpha\sin\alpha\cos\theta\sin\theta\cos\phi) . \end{aligned} \tag{19}$$

The directions of the dipoles are given by the angles $(\theta,\phi)$ and $(\alpha,0)$, and $Q$ is the elastic dipole moment. The parameters $A$ and $B$ are

$$A = \frac{1}{16\pi\mu} \quad \text{and} \quad B = \frac{\lambda+\mu}{\lambda+2\mu} , \tag{20}$$

where $\lambda$ and $\mu$ are the Lamé coefficients. The most stable relative orientation of the dipoles, which minimizes the interaction energy and thus maximizes the magnitude, is for $\alpha=\pi/2$ and $\theta=0$, so we have

$$\Delta\varepsilon \le \frac{1}{16\pi\mu}\left[\frac{4}{3}+\frac{8}{3}\frac{\lambda+\mu}{\lambda+2\mu}\right]\frac{Q^2}{z^3} . \tag{21}$$

As copper is not isotropic there is a slight uncertainty in the values of these coefficients; we choose $\mu=2.4\times10^{11}$ erg/cm$^3$ and $\lambda=1.2\times10^{12}$ erg/cm$^3$. In a metal, dipole moments such as that formed by a divacancy can be expected to have $Q$ with an upper bound $\le 10$ eV. Evaluating Eq. (21) for a dipole spacing of 1.7 nm yields an upper bound on the dipole-dipole interaction energy $\Delta\varepsilon \le 10$ meV. This is considerably less than the 60-meV interaction energy required to change a two-level fluctuation frequency by a factor of 10 at 300 K. And of course many interactions are considerably stronger than this. We conclude that either there is a stronger, longer-range defect interaction mechanism than that arising from the elastic strain field, or, more likely, the randomly distributed, simple dipole-dipole interaction model is not appropriate here.

Strain field interactions involving extended defects are, of course, much longer ranged than the dipole-dipole interaction. For example, the elastic interaction between two parallel dislocation segments of length $L_1$ and $L_2$ and Burgers vectors $\mathbf{b}_1$ and $\mathbf{b}_2$ is given by[25]

$$\begin{aligned} \Delta\varepsilon = &-\frac{2\mu}{4\pi}\int_{L_1}\int_{L_2}(\mathbf{b}_1\times\mathbf{b}_2)\frac{d\mathbf{l}_1\times d\mathbf{l}_2}{\rho} \\ &+\frac{\mu}{4\pi}\int_{L_1}\int_{L_2}\frac{(\mathbf{b}_1\cdot d\mathbf{l}_1)(\mathbf{b}_2\times d\mathbf{l}_2)}{\rho} \\ &-\frac{\mu}{4\pi(1-\nu)}\int_{L_1}\int_{L_2}(\mathbf{b}_1\times d\mathbf{l}_1)\nabla\nabla\rho(\mathbf{b}_2\times d\mathbf{l}_2) \end{aligned} \tag{22}$$

and thus varies as $1/\rho$, if $\rho$, the distance between the segments, is less than $L_1$. Thus by invoking the existence of extended, more complex defect structures, a stronger interaction strength can be justified. However, typically the dislocation density in relatively high-quality metal films is of the order of $10^{10}$–$10^{11}$ per cm$^2$. Transmission electron microscopy examination of a copper film of the type used in the nanobridge experiment indicates a dislocation density at the lower end of this range. The agreement between the $1/f$ noise level in the bulk film and that found in the larger nanobridges, which are of order $(20\text{ nm})^3$ in volume, is rather good, so it would seem appropriate to conclude that, since multiple dislocations (or grain boundaries) are not likely in a volume of this size, dislocation-dislocation interactions are not the major effect.

Since individual dipole-dipole interactions appear to be too weak, and the dislocation density too low to account for the observed TLF interactions, we propose many-body elastic interactions involving multiple defect elements as the most likely explanation for the $1/f$ noise phenomena. The clustering of simple atomic defects as a result of such multiple interactions is a well established occurrence in solids, as exemplified, for example, by the "point-defect atmosphere" that is generally found gathered about dislocations and grain boundaries.[26] The formation of small defect clusters resulting from the mutual attraction of point defects during film growth is also a well-known and extensively studied phenomenon.[27] The scale and range of the elastic interaction between a defect element and an adjacent or surrounding group of defects can be roughly estimated by considering the interaction energy between a point defect and an edge dislocation with Burgers vector $\mathbf{b}$, which, as given by Teodosiu,[25] is

$$\Delta\varepsilon = \frac{-\mu b(1+\nu)\delta v}{3\pi(1-\nu)}\frac{\sin\theta}{\rho} . \tag{23}$$

Here, $\delta v$ is the lattice volume charge introduced by the point defect and $\nu=\lambda/[2(\lambda+\mu)]$ is Poisson's ratio.

Evaluation of $\Delta\varepsilon$ of Eq. (23) using values typical of a vacancy near to an edge dislocation in copper indicates that such an elastic interaction between an element of a defect cluster and the rest of the cluster can indeed provide the required interaction energy over a distance of order 1–2 nm.

As discussed above, the dynamics of the defect fluctuations that are directly observed in the metal nanobridges indicates that, collectively, the defect elements form a defect glass imbedded in the crystalline lattice and that this defect glass is responsible for the existence and microscopic character of the excess low-frequency noise in metal films. This defect glass may well be somewhat inhomogeneous since, as we have noted, defect clusters in the metal can be formed by point-defect segregation during the growth of the film. Nonepitaxial, low-temperature film growth is, of course, a very nonequilibrium process that results in films that are typically under a significant degree of local stress. But the defect glass cannot be so inhomogeneous that there is generally more than one independent defect cluster in a volume the size of a nanobridge. The rarity of truly independent two-level fluctuations at low temperature in the larger nanobridges and the complex defect dynamics above 150 K for the smallest nanobridges demonstrate the participation of the entire defect glass within the nanobridge region in the defect fluctuations. We also note that the defect elements cannot be so close together that they form a completely stable defect complex or that a measurable amplitude modulation results from the TLF interactions.

The implication of this defect-glass model is that the two-level fluctuations should not be viewed as the simple change in position of a fully localized defect, e.g., the rotation of a divacancy dipole, in a perturbed lattice. Instead, in order to account for the observed strength of the interaction between TLF's in the context of elastic strain field interactions, the TLF's should be considered as the result of a collective change in state (or configuration) of a local region of the defect glass. While the measure of the scattering-cross-section change resulting in a TLF is of order atomic dimensions, a local group of interacting defects must collectively participate, to some extent, in this reconfiguration. As we have already noted, to reduce the required activation energy for reversible defect motion in a crystal to well below 1 eV, and to produce a broad distribution of such activation energies, requires the collective effect of a random assembly of defects, which lowers the potential at various points so that local atomic-scale changes, e.g., a dipole rotation, can become thermally activated, while raising the potential elsewhere. From that realization it is not a major leap to suggest that such changes have the participation of a number of defect elements in a given region, i.e., that the reconfiguration is not fully localized to the dipole rotation but includes the "relaxation" of neighboring defect elements. Note that this "relaxation" can include the change in the duty cycle of nearby, weakly bound defects that are fluctuating at a higher rate, as well as the displacement of any mobile impurities (e.g., $H^+$) or point defects that may be in the vicinity. Together these changes can materially change the defect potential seen by the other interaction defect elements. It appears that only such a collective mechanism can provide an elastic interaction of sufficient range to explain the direct experimental observations.

## VIII. SUMMARY AND CONCLUSIONS

The microfabrication of clean metal nanobridges as small as 10–20 atoms across has allowed us to study the microscopic constituents of $1/f$ noise in clean metal films. We find that the $1/f$ noise is due to defect motion as previously suspected. But these microscopic studies have also provided information impossible to obtain from measurement of bulk noise spectra. Typical scattering-cross-section changes of atomic dimensions are observed, with an attempt rate that does not vary strongly for one fluctuation to the next. This noise is not due to defects diffusing through the sample; rather, strong defect-defect interactions produce stationary defects with metastable configurations. As result of the random nature of the defect interactions, the system potential has various low-energy barrier heights for the fluctuation of defect elements between alternative configurations. Measured values of the interaction energy and interaction length are only compatible with a simple model of elastic dipoles and linear elasticity theory if the mean dipolar defect element separation is considerably less than indicated by the direct observation of defect dynamics in our clean nanobridges. This has led us to suggest that elastic interactions bind the defect elements into a defect glass embedded in the crystalline lattice. The many-body interactions between metastable elements with the surrounding defect glass, which might be roughly modeled as an extended defect, are responsible for the large range of activation energies for defect fluctuation required to produce the $1/f$ spectrum and for the constantly evolving nature of the discrete defect fluctuations above the defect-glass melting point.

These results lead directly to the speculation that glassy behavior is in fact far more universal than has previously been discussed, occurring even in samples that, on average, are only moderately disordered. Because the behavior of such properties as the thermal conductivity and the specific heat are dominated by the behavior of the crystalline material, they cannot be used to probe whether or not the disorder displays glassy behavior. The existence of glassy behavior due to small amounts of disorder can only be observed with a technique, such as the microscopic noise measurements discussed here, that does not probe the crystalline material.[28]

These direct observations of individual defect fluctuations, and especially of the dominant role of strong elastic interactions between fluctuating defects in the "glassy" defect system embedded in clean metal films, do appear to have some implications for our understanding of the properties of glasses, particularly at low temperatures. A very successful model for explaining such properties is the tunneling two-level system mode,[29,30] which postulates that because of the disorder of glasses, there are atoms or groups of atoms that can tunnel between two configurations with a fairly high probability. With the

addition of a flat distribution over a broad range of tunneling times, and independent two-level systems, this model serves well to explain such phenomena as the linear specific heat and $T^2$ thermal conductivity found in glasses below 1 K. Although no one has ever actually observed an individual tunneling two-level system in a glass, the predictions of this model have been thoroughly probed by experimentalists. Perhaps the most revealing experiment is that of Golding and Graebner,[31] who observed phonon echoes in response to acoustic pulses in glasses. Such behavior can be explained in analogy with pulsed magnetic-resonance experiments, by postulating that the glass has low-lying excitations that obey spin dynamics. This assumption is easily satisfied with two-level systems, although more than two levels will work just as well. While Golding and Graebner suggested that interactions between two-level systems were too weak to affect any measured properties other than the dephasing time for the "spins," recently Yu and Leggett[32] proposed that adding interactions to the two-level system model of glasses can improve its predictive abilities. Actually they are willing to abandon two-level systems entirely, replacing them with any kind of strongly interacting atomic motion that has a low-energy barrier. In particular, they point out that the two-level system model is hardly unique in its predictive abilities for much of the data for glassy systems, just as we have seen that independent TLF's are not the only way to obtain a $1/f$ noise spectrum. In addition, the two-level system model fails to explain many of the universal features of glassy systems between 1 and 10 K, such as a plateau in the thermal conductivity and a bump in the specific heat. Yu and Leggett adopt a model with the assumptions of a distribution of low-lying energy excitations that are otherwise unspecified and of a strain-mediated dipole interaction between the excitations, and assume further that the interactions are in fact responsible for the spectrum of low-lying modes. Their preliminary estimates suggest that such a model can explain the features of glasses between 1 and 10 K mentioned above, as well as the fact that below 1 K the experimental specific heat is slightly superlinear while the experimental thermal conductivity is subquadratic.

Our noise measurements in the crystalline metal nanobridges show that two-level fluctuations due to reversible atomic reconfiguration are common even in quite clean metal films and are the dominant source of $1/f$ noise in as-prepared metal films. We have directly observed the process whereby interactions between defect elements produce a spread of activation energies for atomic motion and when the density of actively fluctuating defect elements is sufficiently high the result is a constantly evolving defect potential. The interactions observed between fluctuating defects in the nanobridges are quite strong, with $\Delta\varepsilon/\varepsilon$ of order unity, and appear to be explicable only if the mechanism involves collective defect-glass interactions. Of course, there is an important difference between the crystalline metal systems and amorphous glasses in that in the metals that we have been examining the defect density is low; as a result the glass is relatively dilute and the resulting spread in the distribution of defect activation energies does not extend substantially to extremely small energies. But as the average density of atomic defects increases in a metal, the defect-glass atmosphere becomes more dense, until finally the "fully dense" or "uniform" glass state is reached. Such a uniform defect-glass system would then be expected to have a very broad spread in activation energies and result in very-low-energy two-level tunneling states that can be active at low temperature. Palladium samples with typical $1/f$ noise versus temperature as shown in Fig. 3 are the system studied here that appears to be the closest to this uniform defect limit.

While the experiments by Golding and Graebner[31] show that the idea of low-lying excitations with discrete states cannot be discarded entirely, the fluctuation dynamics we observe at high temperatures for defects in nanobridges may be applicable in developing a better understanding of TLF's in more fully disordered systems. The strong interactions we observe between defect fluctuations suggest that although a multilevel description of glasses is still appropriate, interactions between these atomic reconfigurations are important, indeed fundamental, to the formation of the low fluctuation barrier heights in the complex defect potential. The apparent necessity of invoking collective interactions between multiple elements of defect glass to account for the two-level fluctuation interaction strength suggests that an approach that focuses on the interactions between atomic defects and on the view that two-level states are the collective reconfiguration of local regions of the defect system may well be more successful in explaining the diverse low-temperature properties of glasses. Clearly the direct observation of the microscopics of $1/f$ noise in clean metals has produced a wealth of information. Studies of the evolution of this behavior with increased system disorder and the extension of such studies to lower temperatures in much more highly disordered materials should prove equally revealing.

## ACKNOWLEDGMENTS

We thank Leonid Pesenson for his considerable assistance, including very helpful discussions regarding the possible role of extended defects in the generation of $1/f$ noise. We acknowledge the extensive efforts of Tim Shaw in measuring the $1/f$ noise levels of a number of samples and Dan Ralph for his careful reading of the manuscript, extensive advice, insightful comments, and assistance. We thank Neil Zimmerman for making the bulk $1/f$ noise measurements. We also acknowledge Richard Tiberio and others in the National Nanofabrication Facility staff for their contributions to the fabrication of the metal nanobridges. The experimental portion of this research was carried out at Cornell University and was supported in part by the National Science Foundation through the Cornell Materials Science Center and through the National Nanofabrication Facility, and in part by the Office of Naval Research. While at Cornell, K.S.R. received partial support from AT&T.

[1]K. S. Ralls, W. J. Skocpol, L. D. Jackel, R. E. Howard, L. A. Fetter, R. W. Epworth, and D. M. Tennant, Phys. Rev. Lett. **52**, 228 (1984).

[2]C. T. Rogers and R. A. Buhrman, Phys. Rev. Lett. **53**, 1272 (1984).

[3]K. R. Farmer, C. T. Rogers, and R. A. Buhrman, Phys. Rev. Lett. **58**, 2255 (1987).

[4]M. J. Uren, M. J. Kirton, and S. Collins, Phys. Rev. B **37**, 8346 (1988).

[5]A probable exception is magnetic systems; see, for example, N. E. Israeloff, M. B. Weissman, G. J. Nieuwenhuys, and J. Kosiorowska, Phys. Rev. Lett. **63**, 794 (1989).

[6]S. Machlup, J. Appl. Phys. **25**, 341 (1954).

[7]P. A. Lee, A. D. Stone, and H. Fukuyama, Phys. Rev. B **35**, 1039 (1987), and references cited therein.

[8]S. Feng, P. A. Lee, and A. D. Stone, Phys. Rev. Lett. **56**, 1960 (1986).

[9]S. Hershfield, Phys. Rev. B **37**, 8557 (1988).

[10]M. B. Weissman, Rev. Mod. Phys. **60**, 537 (1988).

[11]J. Pelz and J. Clarke, Phys. Rev. Lett. **55**, 738 (1985).

[12]N. M. Zimmerman and W. W. Webb, Phys. Rev. Lett. **61**, 889 (1988).

[13]P. Dutta and P. M. Horn, Rev. Mod. Phys. **53**, 497 (1981).

[14]K. S. Ralls, R. A. Buhrman, and R. C. Tiberio, Appl. Phys. Lett. **55**, 2459 (1989).

[15]K. S. Ralls, D.C. Ralph, and R. A. Buhrman, Phys. Rev. B **40**, 11 561 (1989).

[16]I. K. Yanson, Zh. Eksp. Teor. Fiz. **66**, 1035 (1974) [Sov. Phys. JETP **39**, 506 (1974)].

[17]I. K. Yanson and O. I. Shklyarevskii, Sov. J. Low-Temp. Phys. **12**, 509 (1986) [Fiz. Nizk. Temp. **12**, 899 (1986)].

[18]A.G.M. Jansen, A. P. van Gelder, and P. Wyder, J. Phys. C **13**, 6073 (1980).

[19]A.G.M. Jansen, A. P. van Gelder, P. Wyder, and S. Strassler, J. Phys. F **11**, L15 (1981).

[20]K. S. Ralls, D. C. Ralph, and R. A. Buhrman (unpublished); see also D. C. Ralph, K. S. Ralls, and R. A. Buhrman, in *Nanostructure Physics and Fabrication,* edited by M. A. Reed and W. P. Kirk (Academic, Boston, 1989), p. 453.

[21]K. S. Ralls and R. A. Buhrman, Phys. Rev. Lett. **60**, 2434 (1988).

[22]I. K. Yanson, A. I. Akimenko, and A. B. Verkin, Solid State Commun. **43**, 765 (1982).

[23]N. Giordano and E. R. Schuler, Phys. Rev. B **41**, 11 822 (1990).

[24]E. R. Grannan, M. Randeria, and J. P. Sethna, Phys. Rev. B **41**, 7784 (1990); E. R. Grannan, Ph.D. thesis, Cornell University, 1989.

[25]C. Teodosiu, *Elastic Models of Crystal Defects* (Springer-Verlag, Berlin, 1982).

[26]J. P. Hirth and J. Lothe, *Theory of Dislocations* (Wiley, New York, 1982), Chap. 14.

[27]See, for example, Proceedings of the International Conference on the Properties of Atomic Defects in Metals, Argonne, Illinois, 1976, edited by N. L. Peterson and R. W. Siegel [J. Nucl. Mater. **69/70** (1978)].

[28]N. O. Birge, B. Golding, and W. H. Haemmerle, Phys. Rev. Lett. **62**, 195 (1989) report that the $1/f$ noise magnitude observed in polycrystalline bismuth samples can be explained using a density of two-level states that is appropriate for glasses, further supporting this idea that glassy behavior can be found lurking in crystalline materials.

[29]P. W. Anderson, B. I. Halperin, and C. M. Varma, Philos. Mag. **25**, 1 (1972).

[30]W. A. Phillips, J. Low Temp. Phys. **7**, 351 (1972).

[31]B. Golding and J. E. Graebner, Phys. Rev. Lett. **37**, 852 (1976); J. E. Graebner and B. Golding, Phys. Rev. B **12**, 964 (1979).

[32]C. C. Yu and A. J. Leggett, Comments Condens. Mater. Phys. **14**, 231 (1988).